Fluorine containing self-crosslinking acrylic latexes with reduced flammability and their application as polymer binders for heterogeneous cation-exchange membranes

Jana Machotova [a*], Eliska Stranska [b], Jiri Skornok, [a] Lucie Zarybnicka[a], Klara Melanova[c], Jozef Rychly[d], Adela Ruckerova[a]

[a] *Institute of Chemistry and Technology of Macromolecular Materials, Faculty of Chemical Technology, University of Pardubice, Studentská 573, 532 10 Pardubice, Czech Republic*

[b] *MemBrain, Ltd., Pod Vinicí 87, 471 27 Stráž pod Ralskem, Czech Republic*

[c] *Joint Laboratory of Solid State Chemistry of the Institute of Macromolecular Chemistry of AS CR and University of Pardubice, Faculty of Chemical Technology, University of Pardubice, Studentská 573, 532 10 Pardubice, Czech Republic*

[d] *Fire Research Institute, Ministry of Interior of the Slovak Republic, Rožňavská 11, 83104 Bratislava, Slovakia*

Correspondence to: Jana Machotova; e-mail: jana.machotova@upce.cz, tel.: +420 466 037 194

Abstract

In this study, self-crosslinking core–shell latexes comprising copolymerized perfluorethyl groups and a novel flame retardant based on phosphazene derivative were prepared by the semi-continuous non-seeded emulsion polymerization of 2,2,2-trifluorethyl methacrylate, methyl methacrylate, butyl acrylate, methacrylic acid and hexaallylamino-*cyclo*-triphosphazene as main monomers. For interfacial crosslinking, diacetone acrylamide was copolymerized into the shell layer of latex particles to provide sites for subsequent reaction with adipic acid dihydrazide. The heterogeneous cation-exchange membranes were obtained by dispersing commercial strong acid cation-exchange resin powder in the latex binder and casting the mixture followed by keto-hydrazide crosslinking reaction. It was found that the increased concentration of fluorine atoms and phosphazene units in the macromolecular structure of interfacially

crosslinked emulsion polymers resulted in a significant enhancement of their flame resistance and shape stability in aqueous environment. Moreover, the easily prepared heterogeneous cation-exchange membranes based on latexes with higher amounts of fluorine and phosphazene units were shown to exhibit satisfactory physicochemical and electrochemical properties.

1 Introduction

The research on the development of more effective and more environmental friendly fluorinated polymer products is the mainstream in the field of modern fluorinated materials all the time. Consequently, many researchers have devoted themselves to investigating and developing fluorinated acrylic latexes due to their special surface properties, good adhesion to matrices and environmental protection value. These materials have been used especially as chemical resistant coatings for textile, paper and leather.[1–3] Up to date, fluorinated acrylate polymer emulsions with various structures, such as graft,[4] random, and core–shell[5–9] have been synthesized via diverse emulsion polymerization techniques. Among these materials, core–shell fluorinated acrylic latexes, composed of fluorine-free core and fluorine-containing shell[10–14] were paid much attention, especially as protective and decorative coatings. Considering the extraordinary properties of fluorinated latexes, these materials represent promising products not only in the field of paints but also in other industrial applications.

Separation membranes have become important part of chemical technology because of their growing industrial applications in the areas of biotechnology, nanotechnology and membrane based energy devices in addition to the separation and purification processes. Ion exchange membranes (IEMs) are among the most advanced types of separation membranes which are generally utilized as an active separator in diverse electrically driven processes such as electrodialysis for desalting brackish water, reconcentrating brine from seawater and production of table salt. Additionally, IEMs play an important part in environmental protection, treating industrial and biological effluents, in resource recovery and food and pharmacy processing as well as manufacturing of basic chemical products.[15,16] In IEMs, the charged groups attached to the polymer backbone are freely permeable to opposite sign ions under the influence of the electric field which separates ionic species from aqueous solution and other

uncharged components.[17–19] IEMs are classified, according to their structure and preparation method, into two major categories: homogeneous and heterogeneous.[20,21]

Homogeneous IEMs are prepared mostly by polymerization[22] and heterogeneous IEMs are generally made by mechanical incorporation of powdered ion-exchange resin into extrudable or moldable matrices such as polyethylene, polypropylene, poly(vinylchloride) or acrylonitrile copolymers. Such membranes are usually prepared either by calendaring of ion-exchange particles into an inert plastic binder or dry moulding of inert binder polymers and ion exchange particles and then milling the mould stock.[23] Other rare but possible means of heterogeneous IEMs preparation is either dispersing ion exchange particles in a partially polymerized binder polymer and casting into a film, followed by finishing the polymerization or dispersing ion exchange particles in a solution containing a binder, casting the mixture into a film and evaporating the solvent.[24–27]

A lot of research has already been performed to improve the heterogeneous IEMs´ physico-chemical properties, which resulted in various modification techniques. Variation of functional groups, selection of different polymeric binders, polymer blending, use of various additives, and more uniform distribution of functional groups are important ways to obtain superior IEMs.[28–31] Nevertheless, only poor research activity has been devoted to modifications in terms of heterogeneous IEMs´ preparation based on latex binder.[32,33] In this case, fabrication techniques available to latex such as casting could be used instead of common dry moulding requiring high pressure and temperature, demanding instrumentation and equipment. Latex could be easily used to produce IEMs with geometric versatility, fast production rate and optimal material properties such as high fracture and impact tolerance, low cost and environmental impact. Hence, this study considers easily fabricated heterogeneous IEMs based on ion-exchanging resin particles and fluorinated film-forming latex binder in contrast to traditional heterogeneous IEMs based on polyolefin binder fabricated using moulding or calendaring techniques.

As crosslinking is an effective and simple method to enhance shape stability and mechanical qualities of IEMs, in particular, to limit their overfull water swelling,[34] the self-crosslinking mechanism was introduced into the latexes. Among different crosslinking reactions, the keto-hydrazide self-crosslinking has been studied extensively.[35–39] The latexes based on diacetone acrylamide (DAAM) and adipic acid dihydrazide (ADH) self-crosslinking system are usually composed of core–shell

particles with DAAM repeat units incorporated into the polymer backbone of the shell layer. These latexes can get cured rapidly at ambient temperature and do not need any additional crosslinker to be added before use. The reaction between the carbonyl functionalities of DAAM and hydrazide groups of ADH is favored by the loss of water and the simultaneous decrease in pH arising from the evaporation of ammonia or amines during the film forming process.[40] The network formation mechanism based on the keto-hydrazide crosslinking reaction is depicted schematically in Fig.1.

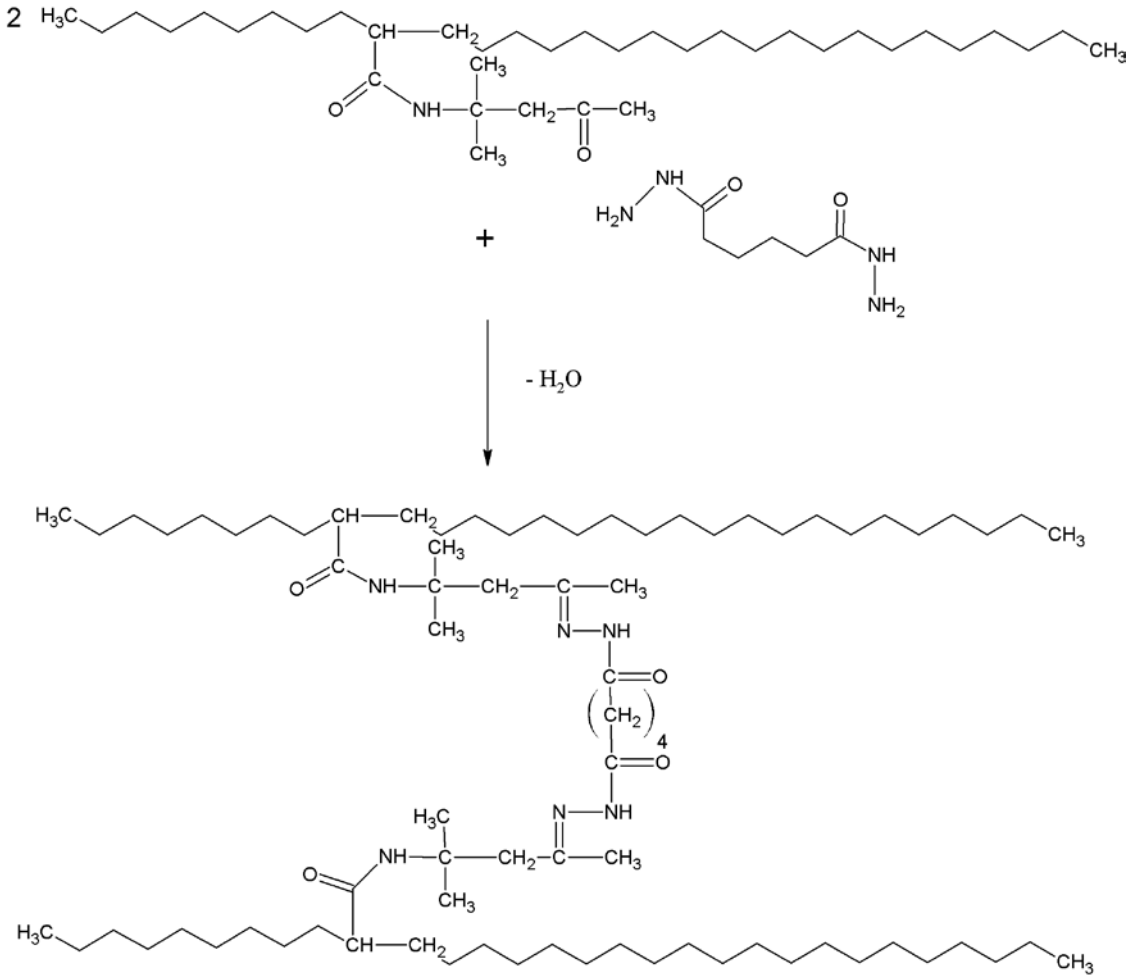

Figure 1: Scheme showing the crosslinking reaction of ketone carbonyl groups with adipic acid dihydrazide.

The electrochemical separation processes occasionally suffer from the increased risk of flame, especially at high currents and voltages. [41–43] Thus, local heating of the IEM may occur resulting in sparks formation due to IEMs charging. Hence, the current study is focused on flame-resistant self-crosslinking acrylic latexes bearing in their polymeric chains covalently linked units of 2,2,2-triflouroethyl methacrylate (TFEMA) and hexaallylamino-*cyclo*-triphosphazene (HACTP) (being proved as the effective

flame retardant for latex coatings[44]) and their application as an alternative binder material with sufficient flame stability for easily fabricated heterogeneous IEMs. The free-standing membranes were obtained by dispersing commercially available cation-exchange particles in the self-crosslinking latex and casting the mixture followed by keto-hydrazide crosslinking reaction. The physicochemical and electrochemical properties of the prepared heterogeneous IEMs were compared to a commercial heterogeneous cation-exchange Ralex® membrane.

2 Experimental

2.1 Materials

Allyl amine and hexachloro-*cyclo*-triphosphazene (HCCTP) were used for the synthesis of the hexaallylamino-*cyclo*-triphosphazene (HACTP) flame retardant and were purchased from Sigma-Aldrich, Czech Republic. Self-crosslinking latexes investigated in this research work were synthesized of 2,2,2-trifluoroethyl methacrylate (TFEMA), methyl methacrylate (MMA), butyl acrylate (BA), methacrylic acid (MAA), and diacetone acrylamide. All the monomers were purchased from Sigma-Aldrich (Czech Republic). Disponil FES 993 IS (BASF, Czech Republic) was used as the surfactant and ammonium persulfate (Penta, Czech Republic) was utilized as the initiator of the polymerization reaction. Adipic acid dihydrazide (ADH) was utilized as the crosslinker and was purchased from Sigma-Aldrich (Czech Republic). Tetrahydrofuran (THF, Penta, Czech Republic) was stored under anhydrous conditions using activated molecular sieves. All the chemicals were utilized as received without any further purification. Suqing 001 x 7 Na (Jiangsu Suqing Water Treatment Engineering Group Co., China) strong acid cation exchange resin powder based on polystyrene matrix, containing sulfonyl groups was utilized as the functional group agent for IEMs preparation. Ralex® CM(H) heterogeneous cation-exchange membrane (Mega, Czech Republic) was used as the comparative sample.

2.2 Preparation of self-crosslinking latexes

Self-crosslinking latexes of core–shell particles containing various levels of TFEMA and HACTP in their core and shell structures were synthesized by the semi-continuous non-seeded emulsion polymerization comprising a variable content of monomers (see Table 1). The preparation and characterization of HACTP flame retardant has been described in detail in the reference.[44] The synthesis reaction is shown briefly in Fig. 2. The prepared HACTP was shown to be readily soluble in the utilized

acrylic monomers and was incorporated into shell and core–shell structure of latex particles, respectively. Similarly, TFEMA was copolymerized into shell and core–shell structures of latex particles, respectively. The core/shell weight ratio of latex particles was 1/1, which means a shell thickness about 10 % of the particle diameter. The nature of acrylic monomers forming core and shell phases was chosen to achieve a calculated T_g (using the Fox equation[45]) of approximately 5 °C. The shell layer included a constant amount of DAAM repeat units to provide ketone carbonyl functionalities for interfacial crosslinking by reaction with ADH added during latex formulation. Carboxyl functionalities which were introduced into the structure of core and shell layers by copolymerization with a constant amount of MAA into all the prepared copolymers, were supposed to have three functions: (i) to improve the colloidal stability of latexes (ii) to ensure the acid catalysis of keto-hydrazide crosslinking reaction and (iii) to support the cation-exchanging ability of the resulting binder polymer.

Table 1

Composition and characteristics of self-crosslinking latexes based on core–shell particles containing TFEMA and HACTP

Sample	Composition of monomer feeds (wt.%) TFEMA/MMA/BA/MAA/DAAM/HACTP		Particle size in the water phase (nm)		Viscosity (mPa.s)*	MFFT (°C)
	Core	Shell	Core	Core–shell		
C_0S_0	0/50/48/2/0/0	0/41/50/4/5/0	102	124	5.2	6.9
$C_0S_{0.5}$	0/49.5/48/2/0/0	0/40.5/50/4/5/0.5	94	116	8.3	7.7
$C_{0.5}S_{0.5}$	0/49.5/48/2/0/0.5	0/40.5/50/4/5/0.5	96	120	6.7	7.1
C_0SF_0	0/50/48/2/0/0	47.5/0.5/43/4/5/0	116	142	9.9	7.6
$C_0SF_{0.5}$	0/50/48/2/0/0	47.5/0/43/4/5/0.5	107	135	8.8	7.6
$C_{0.5}SF_{0.5}$	0/49.5/48/2/0/0.5	47.5/0/43/4/5/0.5	100	122	4.1	6.8
CF_0SF_0	56.5/0.5/41/2/0/0	47.5/0.5/43/4/5/0	108	131	5.3	7.5
$CF_0SF_{0.5}$	56.5/0.5/41/2/0/0	47.5/0/43/4/5/0.5	106	129	6.8	8.6
$CF_{0.5}SF_{0.5}$	56.5/0/41/2/0/0.5	47.5/0/43/4/5/0.5	113	138	7.0	7.8

* Value obtained after 6-months storage at room temperature (23 ± 2 °).

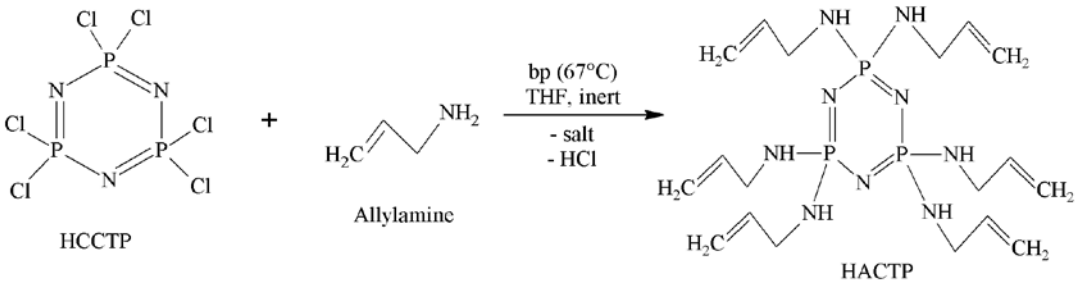

Fig. 2. Schematic representation of the synthesis reaction of hexaallyamino-*cyclo*-triphosphazene (HACTP).

The latexes were produced in a 700 mL glass reactor under nitrogen atmosphere at 85 °C. The reactor charge was put into the reactor and heated to the polymerization temperature. Then the monomer emulsion was fed into the stirred reactor at the feeding rate about 2 mL/min in two steps (1. core preparation, 2. shell preparation). After that, during 2 hours of hold period the polymerization was completed. The recipe of emulsion polymerization is shown in Table 2. The pH was adjusted to 8.5 with ammonia solution. To produce the self-crosslinking latexes, a 10 wt.% aqueous solution of ADH, in the amount corresponding to the molar ratio ADH:DAAM = 1:2, was added to the latex with agitation. The solids content of final latexes was about 30 wt.%.

Table 2
Recipe of emulsion polymerisation

Reactor charge:	
Water (g)	150
Disponil FES 993 IS (g)	0.5
Ammonium persulfate (g)	0.4
Monomer emulsion (core):	
Water (g)	160
Disponil FES 993 IS (g)	7.3
Ammonium persulfate (g)	0.4
Monomers (g)	100
Monomer emulsion (shell):	
Water (g)	160
Disponil FES 993 IS (g)	7.3
Ammonium persulfate (g)	0.4
Monomers (g)	100

2.3 Testing of emulsion copolymers

The structure of prepared polymers from the point of view of the copolymerized TFEMA, HACTP and keto-hydrazide crosslinking was investigated by means of a Fourier transmission infrared (FT-IR) spectroscopy on a Nicolet IS50 instrument (Nicolet Companies, USA) with an integrated diamond ATR FT-Raman module. The measurements were performed in the range from 4000 cm^{-1} to 500 cm^{-1}.

The presence of the copolymerized HACTP in the emulsion copolymers was investigated using $^{31}P(H)$ NMR as well. Before NMR analysis, 24-hr THF extraction of dried copolymer samples without ADH addition was performed. Both the high-molar mass polymer material (gel fraction) and the low-molar mass soluble material (sol fraction) were analyzed and compared. The presence of HACTP in sol fraction was determined using a Bruker Advance DRX 300 instrument (Bruker Corp., Germany) at the frequency of ^{31}P: 202.46 MHz and 85 % H_3PO_4 (as the external standard), whereas the incorporation of HACTP in the gel fraction was studied by means of $^{31}P(H)$ NMR using a Bruker Advance III(tm) spectrometer (Bruker Corp., Germany) at the frequency of ^{31}P: 500 MHz equipped with MAS VTN 500SB BL4 N-P/F-H probe. The samples were filled into 4 mm ZrO_2 rotor with the rotation speed 10 kHz. The hydrogen atoms splitting were not observed because of using zgig - inverse-gated decoupling program.

For the glass transition temperature (T_g) and gel content measurements of the synthesized emulsion copolymers without proceeding the self-crosslinking reaction, specimens were prepared by pouring the latexes without ADH crosslinker into a silicone mould. Films were formed by water evaporation at room temperature for a month. T_g values were determined by means of differential scanning calorimetry using a Pyris 1 DSC instrument (Perkin-Elmer, USA). The measurements were carried out at the heating rate of 10 °Cmin^{-1} with N_2 atmosphere. The testing temperature range was -80 to 120 °C. The gel content was determined according to CSN EN ISO 6427 using a 24-hr extraction with THF in a Soxhlet extractor. Around 1 g of the dried latex sample was put into the thimble. After the extraction, the thimble was dried in an oven at 75 °C for 6 h, cooled in a desiccator overnight, and the gel content was calculated from the initial and final weights, assuming that the gelled material remained in the thimble.

2.4 Testing of self-crosslinking latex polymer binders

The apparent viscosity of final self-crosslinking latexes was measured by CSN ISO 2555 using a Brookfield viscometer, Model DV-1 at 100 rpm at 23 °C. The average

particle sizes of structured latex particles in the water phase were obtained from dynamic light scattering (DLS) experiments performed using a Coulter N4 Plus instrument (Coulter, Corp., UK). The DLS measurements were conducted at 25 °C. The concentration of the measured polymer dispersion was approximately 0.05 wt.% of solids.

The morphology of latex particles was observed using transmission electron microscopy (TEM) analysis which was carried out on a JEOL JEM 3010 microscope (JEOL, USA) with an acceleration voltage of 300 kV (LaB6 cathode, point resolution 1.7A) using an energy dispersive X-ray detector (Oxford Instruments, UK). Samples were diluted to 3 wt.% of solids and then stained with 2% phosphotunstic acid solution. One drop of diluted latex was placed onto copper grid and allowed to dry.

The minimum film-forming temperature (MFFT) was measured using the MFFT-60 instrument (Rhopoint Instruments, UK) according to ISO 2115. The MFFT is defined as the minimum temperature at which a film cast from the polymer dispersion becomes continuous and clear. Glass transition temperature (T_g) and gel content values of the synthesized self-crosslinking latexes (after ADH addition) were determined in the same manner as described above.

For evaluating the water swelling of crosslinked latex binder materials, specimens were prepared by pouring the self-crosslinking latexes into a silicone mould. Films were air-dried at room temperature (23 °C) for a month. The water swelling, expressed in terms of water absorption by latex films was measured by immersing samples in distilled water at 23 °C. The water absorption, A is given by $A = 100(w_t - w_0)/w_0$, where w_0 is the sample weight before immersion and w_t is the sample weight after immersion in water during given time. The swollen films were carefully removed from water, and water from the film surface was wiped by touching the polymer with a filter paper. For each sample, three specimens of the approximate dimensions 20 × 20 × 0.75 mm^3 were tested and averaged values of the results were collected as a function of time.

The flammability of crosslinked latex polymers was investigated by means of the dual cone calorimeter (Fire Testing Technology, UK). For the measurements, specimens of dried latex samples of approximate dimensions 80 x 50 x 4 mm^3 were prepared by pouring the self-crosslinking latexes into a silicone mould. Films were air-dried at room temperature (23 °C) for a month followed by vacuum drying at 25 °C for 14 days. The measurements were performed in a sample holder suitable for testing of thermally thin materials. The centre of a measured sample was situated 6 cm from the lowest part of the cone heater. The heat release rate was calibrated by burning methane. The cone

radiancy 25 kWm^{-2} corresponds to a cone temperature 680 °C. It was set from the calibration diagram for a distance of the sample from the cone edge 6 cm.[46] For each sample, three specimens were tested and averaged values of the results were collected.

2.5 Preparation and testing of heterogeneous IEMs

Heterogeneous cation exchange membranes were prepared by casting technique using commercial cation-exchange resin powder as the functional group agent and self-crosslinking latex as the polymer binder. In order to undertake the IEM preparation, cation-exchange resin particles were dried in oven at 30 °C for 48 h and then pulverized into fine particles in a ball mill and sieved to the desired mesh size. The ion exchange resin with desired particle size (10–35 μm) was used in membrane fabrication. The IEMs were obtained by mixing the cation-exchange particles in an amount of 50 wt.% (based on total IEM solids content) in the latex binder using the ULTRA-TURRAX T25 disperser (IKA, Germany) followed by removing air bubbles in a centrifuge. Xylene in a concentration of 5 wt.% (based on total IEM solids content) was used as a coalescing agent. The films with a wet thickness of 750 μm were cast on silicone panels by drawing the resulting mixture using a blade applicator. To prevent any inaccuracy of final IEMs properties (which may result from the incomplete coalescence and/or water entrapment inside the IEM), the IEMs were air-dried at room temperature (23 °C) for a month, although in practice, a procedure of 2 days-long drying at room temperature ensures the production of IEMs that exhibit a sufficient shape stability and readiness for immediate use.

The IEMs were tested according to variation of thickness after swelling in water, ion-exchange capacity (IEC), electrical resistance and permselectivity. The resulting physicochemical and electrochemical properties were compared to the commercial Ralex® CM(H) heterogeneous cation-exchange membrane. The difference between dry and swelled membrane thickness was determined after immersion of the tested membrane in demineralised water for 12 hours at ambient temperature.

IEC of an IEM was determined in the following manner: 1 g of the membrane sample was treated with 50 mL of 0.1 M NaOH, then the sample was left on a shaker for 1 hour at room temperature. Thereafter, for the actual determination, 10 mL of the solution was pipetted and diluted to 30 mL with demineralized water and the sample was titrated with 0.1 M HCl and the equivalence point was determined using phenolphthalein indicator. IEC of the IEM per gram of dry matter was calculated using the following relation:

$$\mathrm{IEC} = \frac{(C_{\mathrm{NaOH}} - (C_{\mathrm{HCl}} \times V_{\mathrm{HCl}})/V^{I}_{\mathrm{NaOH}}) \times V_{\mathrm{NaOH}}}{m} \qquad (1)$$

where V_{HCl} is the volume of HCl solution, C_{NaOH} is the concentration of NaOH solution, C_{HCl} is the concentration of HCl solution, V^{I}_{NaOH} is the consumed amount of the solution for titration (10 mL), V_{NaOH} is the added amount of 0.1 M NaOH (50 mL) and *m* is the weight of dried membrane sample.

The electrical resistance is practically important due to its relation with energy consumption in the process. Before the measurement of the specific resistance (R_s) and the areal resistance (R_A) of a membrane, a membrane sample was equilibrated in a solution of 0.5 M NaCl for 24 hours. The resistance was measured at room temperature in 0.5 M NaCl in the test cell (Fig. 3) using a compensation method. The test cell consisted of two parts which are separated from one another by the IEM sample. Constant direct current of 10 mA was set between interposed platinum electrodes and voltage was measured between reference calomel electrodes at 25 °C. The specific resistance was determined according to the relationship:

$$R_s = \frac{(U_{\mathrm{IM+sol}} - U_{\mathrm{sol}})}{I} \cdot \frac{S}{th} \qquad (2)$$

where R_s is the specific resistance of IEM, $U_{\mathrm{IM+sol}}$ is the potential of a solution with the embedded IEM sample, U_{sol} is the potential of a solution without inserting IEM sample, *I* is the direct current, *S* is the active area of IEM sample of 0.785 cm^2 and *th* is the thickness of IEM sample.

The areal resistance was determined using the relationships:

$$R_A = R_s . th \qquad (3)$$

$$R_r = \frac{|U_{\mathrm{meas}}\,(1,2) - U^{r}_{\mathrm{as}}\,(2,2)|_j + |U_{\mathrm{meas}}(2,1) - U^{r}_{\mathrm{as}}(2,1)|_j}{2I} \qquad (4)$$

where U_{as} is the assymetric voltage and U_{meas} is the measured voltage.

The permselectivity (*P*) that indicates the proportion of the charge transferred from the counter ions to the total transferred charge was determined according to Henderson.[47] Membrane samples were equilibrated in 0.5 M KCl for 24 hours before the measurement. 0.1 and 0.5 M KCl solution were poured into separate parts of the test cell. Permselectivity was subsequently determined according to the relationship:

$$P = \frac{U_{\mathrm{meas}}}{U_{\mathrm{teor}}} \times 100\ (\%) \qquad (5)$$

where U_{meas} is the measured voltage and U_{teor} is the theoretical voltage based on Nernst's law expressed by the relationship (5), with regard to the activity of cations a_{K1}, a_{K2} and anions a_{A1}, a_{A2} in KCl solution present in separate parts of the test.

$$U_{\text{teor}} = -\frac{RT}{2F} \times \ln \frac{a_{K1} \times a_{A1}}{a_{K2} \times a_{A2}} \qquad (6)$$

where R is the universal gas constant = 8.3145 J/mol K, T is temperature (K) and F is the Faraday constant = 96 485 C mol^{-1}.

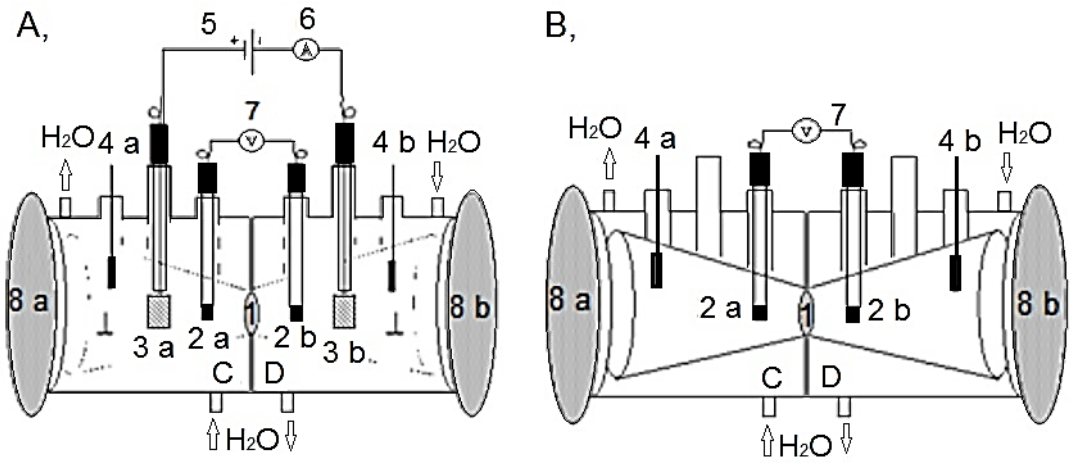

Fig. 3. Schematic representation of the test cell for measuring the electrical resistance (A) and permselectivity (B): C,D – conical vessels containing NaCl solution; 1 – sample of IEM; 2a, 2b – reference calomel electrodes; 3a, 3b – platinum electrodes; 4a, 4b – temperature sensors; 5 – a source of direct current; 6 – ampermeter; 7 – voltmeter; 8a, 8b – clamping plates.

3 Results and discussion

3.1 Characterization of emulsion copolymers

The structure of the prepared copolymers was investigated by means of FT-IR spectroscopy. FT-IR spectra of a representative copolymer containing TFEMA and HACTP without ADH addition (curve a) and after ADH crosslinking (curve b) are shown in Fig. 4. It is evident that both spectra exhibit the similar character. Stretching vibrations of C–H_x groups (x = 1–3) were found between 2873 and 2961 cm^{-1}. Bands of deformation vibrations of C–H_x groups (x = 1–3) occurred in the region of 1394 to 1449 cm^{-1}. The absorption peak at 1735 cm^{-1} was assigned to the characteristic absorption

band of C=O bonds (mainly from TFEMA, MMA and BA) and the absorption peak of N–H bonds at 1537 cm^{-1} indicates that DAAM was copolymerized with acrylic monomers. It can be seen in both spectra as well that the P–N cycle vibration was located at 1168 cm^{-1} and the stretching vibration and wagging vibrations of the C–F bonds were detected at 1280 and 652 cm^{-1}, respectively, which reveals clearly that HACTP and TFEMA took part in the polymerization. When comparing the spectra of the copolymer without and after ADH crosslinking, the absorption peak at 1652 cm^{-1} corresponding to N=C bonds can be observed in the case of ADH-crosslinked copolymer (curve b), which confirms that the keto-hydrazide crosslinking reaction has proceeded.[40,48]

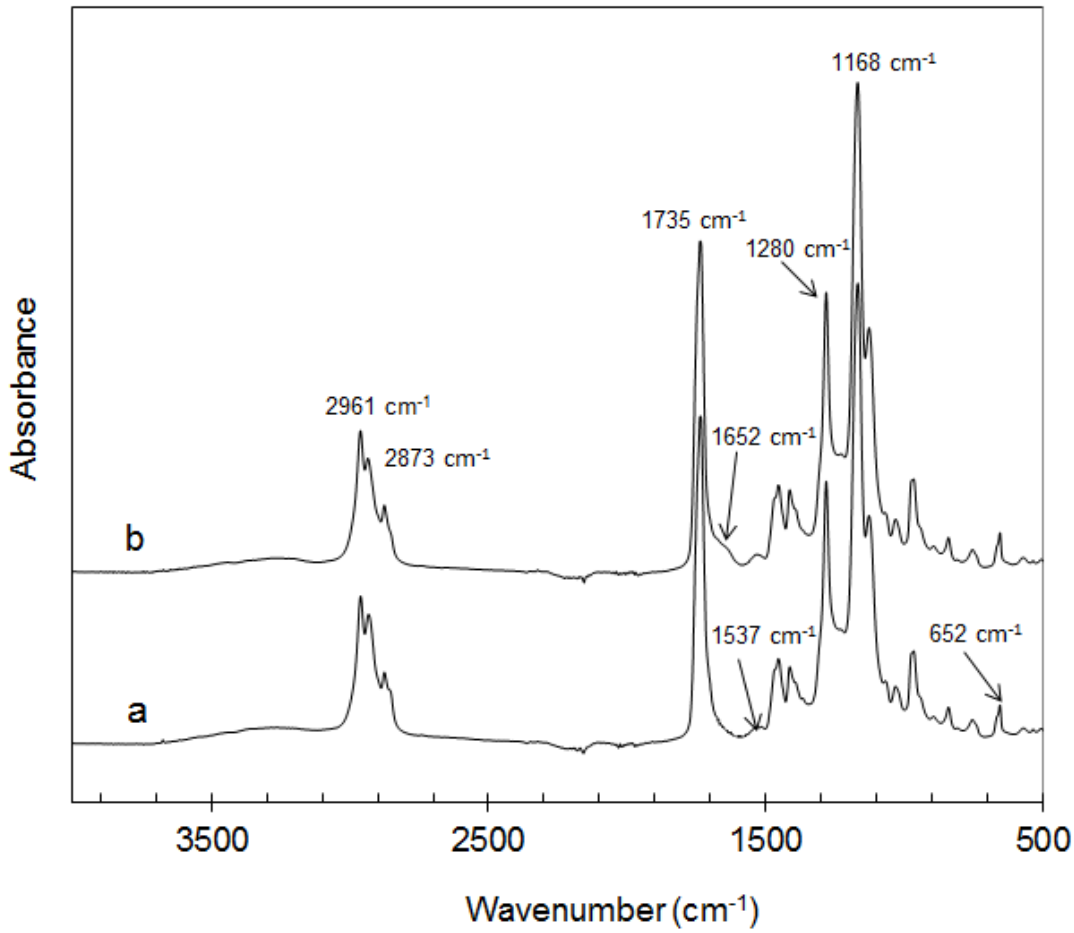

Fig.4. FT-IR spectra of $C_0SF_{0.5}$ copolymer containing TFEMA and HACTP in monomer feeds forming the shell layer of latex particles: (a) sample without ADH addition; (b) sample after ADH crosslinking.

Further, the presence of the copolymerized HACTP in the synthesized emulsion copolymers was verified using $^{31}P(H)$ NMR. Two representative copolymers, namely $CF_0SF_{0.5}$ (containing theoretically 0.5 wt.% of phosphazene derivative in the shell

structure of latex particles) and $CF_{0.5}SF_{0.5}$ (bearing theoretically 0.5 wt.% of HACTP both in the core and shell structures of latex particles) were investigated. It was found for both tested samples that the spectra of their corresponding sol fractions showed the absence of phosphazene derivative, whereas almost the identical ^{31}P NMR spectra were obtained in the case of gel fractions of both investigated emulsion copolymers; the exemplary spectrum of the $CF_{0.5}SF_{0.5}$ gel copolymer is shown in Fig. 5. It can be seen that a singlet at a chemical shift δ (*S*) = 21.52 ppm occurred in the spectrum of the high-molar mass polymer fraction, which indicates the presence of HACTP molecules. Hence, it can be stated that HACTP was covalently bonded into the macromolecular structure of acrylic emulsion polymers.

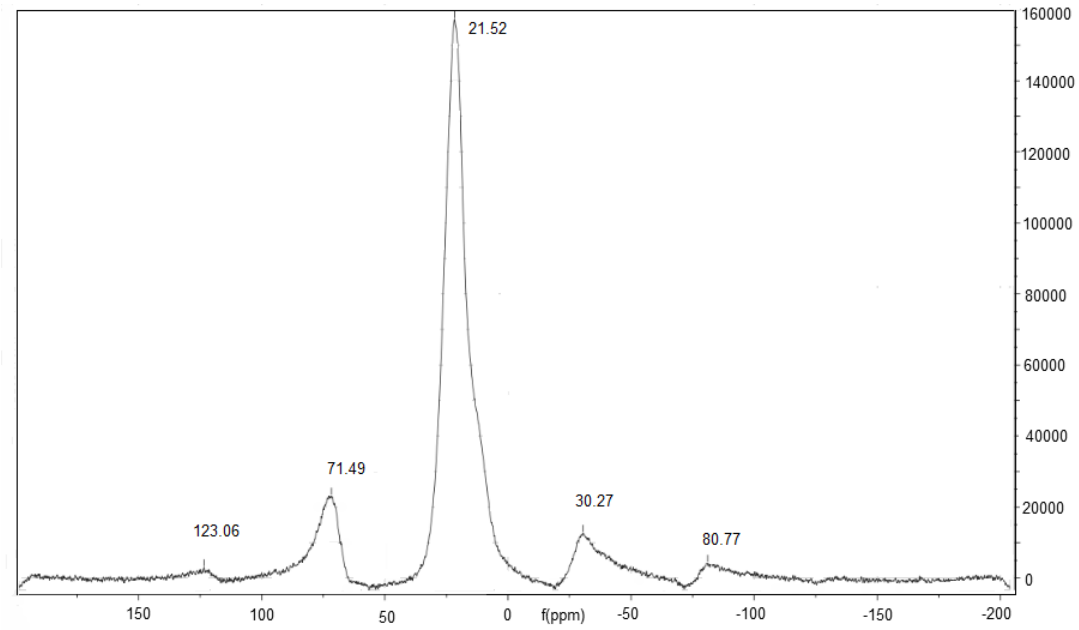

Fig. 5. $^{31}P(H)$ NMR spectrum for the gel fraction of the $CF_0SF_{0.5}$ copolymer containing theoretically 0.5 wt.% of HACTP in the shell structure of latex particles.

The prepared latex copolymers were studied from the point of view of glass transition temperature and gel content with respect HACTP concentration and location inside the latex particles. These characteristic properties are presented in Table 3. In the case of all emulsion copolymers, T_g and gel content values were shown to be influenced particularly by the content of HACTP in latex particles. Although the pendant allyl double bonds of HACTP were supposed to remain partly unreacted (because of steric hindrance effects and lower reactivity in comparison to vinyl groups of acrylic monomers) and therefore the crosslinking ability of the phosphazene derivative was believed to be suppressed, the glass transition temperature and gel content of emulsion

copolymers were found to be increased with the growing content of HACTP. This phenomenon clearly reveals the formation of polymer network and leads us to suppose that in the process of emulsion polymerization of acrylic monomers, HACTP may act as an efficient pre-coalescence crosslinker leading to the formation of latex particles of microgel structure. When comparing the results of the gel content for the emulsion copolymers before and after post-crosslinking by ADH, the ADH-crosslinked copolymers exhibited increased T_g and gel content values as a result of increasing the network density owing to keto-hydrazide crosslinking.

Table 3

Effect of HACTP and post-crosslinking using ADH on T_g and gel content values of emulsion copolymers

Sample	HACTP content (wt.%)		Copolymers without ADH		Copolymers after crosslinking with ADH	
	Core	Shell	T_g (°C)	Gel content (%)	T_g (°C)	Gel content (%)
C_0S_0	0	0	18.3	8.7±1.1	24.6	72.1±1.3
C_0 $S_{0.5}$	0	0.5	21.4	77.9± 0.7	26.0	89.2±0.9
$C_{0.5}S_{0.5}$	0.5	0.5	23.9	83.9±1.1	28.9	98.8±0.5
C_0SF_0	0	0	15.0	7.4±0.9	19.1	75.0±1.2
$C_0SF_{0.5}$	0	0.5	17.1	73.6±1.0	20.3	91.7±0.8
$C_{0.5}SF_{0.5}$	0.5	0.5	17.8	85.6±1.3	22.0	97.4±1.7
CF_0SF_0	0	0	13.9	7.9±0.8	16.1	74.3±0.4
$CF_0SF_{0.5}$	0	0.5	14.4	76.2±1.5	16.8	92.5±1.0
$CF_{0.5}SF_{0.5}$	0.5	0.5	15.2	84.0±1.7	17.9	98.6±0.7

3.2 Properties of self-crosslinking latex polymer binders

Latexes with negligible amount of coagulum (0 – 0.4 %) were synthesized by the semi-continuous non-seeded emulsion polymerization process with varying amount and location of TFEMA and HACTP molecules in core–shell compositions. All the prepared self-crosslinking latexes (after ADH addition) were stable for over 12 months. They were evaluated from the point of view of particle size in the water phase, minimum film-forming temperature and viscosity. These characteristic properties are listed in Table 1. For proving the core–shell morphology of latex particles, the diameters of core particles (samples taken after finishing the core polymerization step) and resulting core–shell particles were determined. Diameters of core particles varied from 94 to 116 nm, whereas particle sizes of core–shell particles were between 116 – 135 nm. When comparing the results between core and core–shell particles for individual samples, they were in a good accordance with the calculated dimension of shell thickness about 10 % of the particle diameter. The DLS results indicated further that the latex particle size was not affected significantly by the composition of emulsion copolymers. Similarly, viscosity of self-crosslinking latexes was shown not to be influenced by the composition of emulsion copolymers.

The core–shell structure of latex particles was verified by TEM analysis as well. All samples exhibited similar character, therefore only one representative TEM image of the sample $C_0SF_{0.5}$ is demonstrated in Fig. 6. It can be seen that the particles were spherical and their sizes were of 80–90 nm in diameter. The core–shell morphology can be evidenced by the difference in contrast between the outer and inner portion of the particles. The light grey inner portion of the latex particle is the acrylic core layer, and the dark outer layer is the HACT-crosslinked shell polymer composed mainly of TFEMA and BA. The clear phase separation between the core and shell phases indicates that the shell monomers have reacted predominantly on the core of particle surface and a well-defined core–shell morphology of latex particles was achieved during the two-step synthesis. Comparing the diameters of latex particles from DLS and TEM analyses, the mean particle sizes in water phase were found to be higher than the corresponding particle sizes in the dry state, which corresponds to solvation and swelling of latex particles by water molecules.

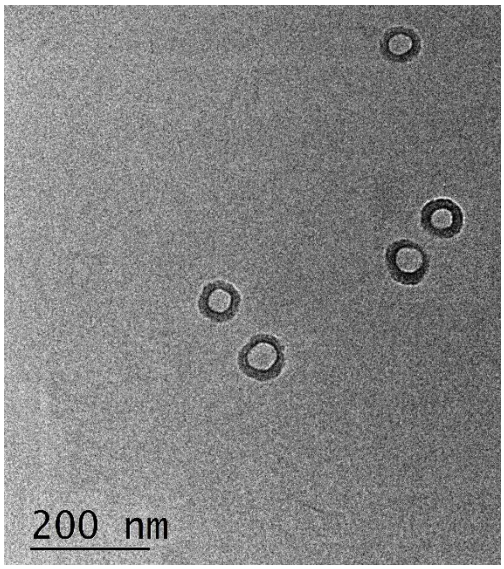

Fig. 6. TEM image of core–shell latex particles $C_0SF_{0.5}$.

On the contrary, the increasing content of HACTP units emulsion copolymers was shown to cause the enhancement of MFFT values of self-crosslinking latexes. This effect (reflecting suppressed coalescence ability of latex particles during film-formation process) is probably connected with increased polymer network density inside latex particles owing to HACTP crosslinking (see Table 3, column representing gel content values). As a result of the restrained segmental mobility, interdiffusion of polymer chains and deformation of latex particles proceeding at coalescence stage were impeded and the higher MFFT values were obtained. Nevertheless, all the tested self-crosslinking latexes exhibited sufficiently low MFFT values being below room temperature, which predetermines good application and film-forming properties.

As heterogeneous IEMs designed for aqueous separation and purification processes should exhibit sufficient shape stability, the ADH-crosslinked latex binder materials were tested from the point of view of water swelling as well. Figure 7 demonstrates that TFEMA and HACTP presence and concentration in emulsion copolymers affected significantly water sensitivity (expressed in terms of water absorption) of the resulting materials. As expected, the increased concentration of perfluorethyl hydrophobic groups in emulsion copolymers resulted in decreased water absorption. This effect was observed most distinctly in the case of materials based on latex particles without HACTP-crosslinking (compare ○ curves in pictures A, B and C). In contrast to the HACTP-free materials (○ curves), water sensitivity of binders comprising the novel phosphazene derivative was decreased with the growing concentration of HACTP in emulsion copolymers (■ curves representing materials

containing HACTP in the shell structure of latex particles and × curves belonging to materials containing HACTP in core and shell layers of latex particles). The pronounced decrease in water swelling was shown especially in the case of fluorine-free binders $C_0S_{0.5}$ (HACTP copolymerized in shell layer of latex particles), $C_{0.5}S_{0.5}$ (HACTP incorporated into core and shell layers) and fluorine-containing binders, namely $C_{0.5}SF_{0.5}$ and $CF_{0.5}SF_{0.5}$. The explanation of this fact may consist in suppressed coalescence of latex particles that were crosslinked during their synthesis with HACTP (acting as the effective pre-coalescence crosslinker). As the result of the restrained inter-particle diffusion of polymer chains and deformation of latex particles proceeding at the coalescence stage, the open film structure was formed and the extraction of emulsifier and other water soluble components by water was facilitated, which resulted in a lower water uptake due to decreased osmotic pressure.[49] This effect was demonstrated clearly especially in the case of ADH-crosslinked $C_0S_{0.5}$ and $C_{0.5}S_{0.5}$ binder materials (■ and × curves in the picture A) that exhibited increased water uptake at early stages of immersion in water followed by a drop in water absorption at later stages of the swelling test. Nevertheless, the highly open film structure of these samples was probably caused not only by HACTP-crosslinking but also as a result of increased glass transition temperatures of these materials (see Table 3). When comparing T_g values of all prepared ADH-crosslinked emulsion copolymers containing HACTP crosslinker, these two samples exhibited T_g values significantly higher than the film-drying temperature (23 °C).

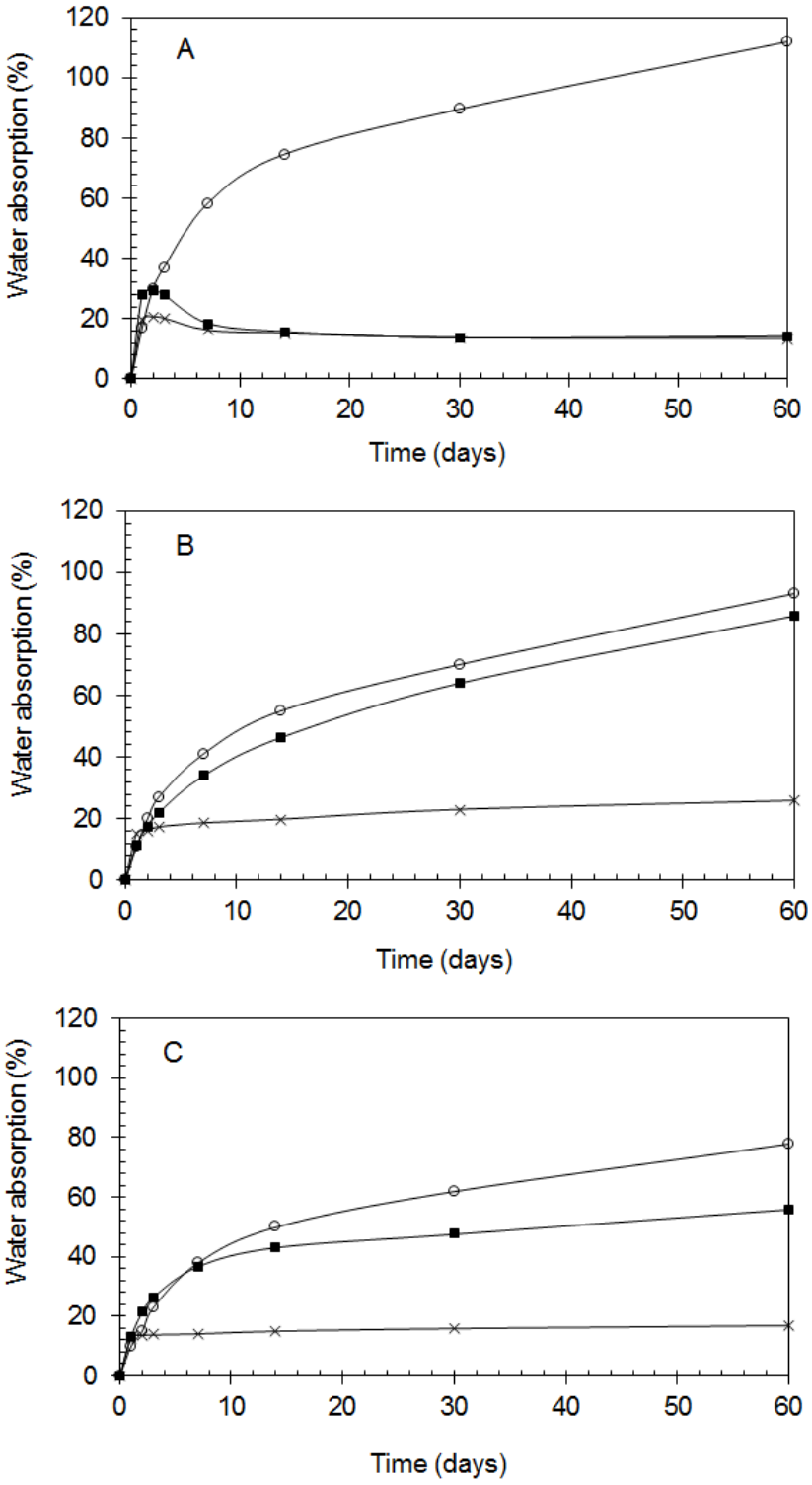

Fig. 7. Water absorption into crosslinked latex binders: (A) materials without TFEMA, (B) TFEMA being copolymerized in the shell layer of latex particles, (C) TFEMA being copolymerized in core and shell layers of latex particles; ○ curves – copolymers without HACTP, ■ curves – copolymers containing HACTP in the shell structure of latex particles, × curves – copolymers containing HACTP in core and shell layers of latex particles. The standard deviations of performed measurements did not exceed 3 %.

3.3 Flammability of self-crosslinking latex polymer binders

Our object of interest was focused also on the evaluation of flame stability of the prepared ADH-crosslinked latex polymers as the alternative binder materials with enhanced flame stability for various applications demanding enhanced flame resistivity. The effect of HACTP and TFEMA amount and location inside latex particles on combustion of ADH-crosslinked latex binders was compared to polyethylene that is a commonly utilized polymer and a conventional binder for commercial heterogeneous IEMs as well. The results obtained from measurements using dual cone calorimeter are presented in Fig. 8 and Table 4. Fig. 8 depicts that TFEMA and HACTP presence and concentration in emulsion copolymers affected significantly flame stability of the resulting materials, especially from the point of view of time to their ignition and character of the heat release rate (HRR) curve. It was shown that latex binders ignited pronouncedly later with the presence of TFEMA in emulsion copolymers (picture A: compare the reference curve (a) of the fluorine-free copolymer C_0S_0 with curves (b) and (c) of samples C_0SF_0 and CF_0SF_0, respectively). This phenomenon can be based on the fact that fluorine-containing acrylic monomer TFEMA was polymerized in the shell of latex particles and the perfluorethyl groups containing the C–F bond with high bond energy in the shell could shield and protect the non-fluorinated polymer segments beneath them. Thus, the flame stability of latex polymers was probably improved mainly due to the introducing of C–F bonds in the shell of latex particles.[12]

The content of HACTP flame retardant in emulsion copolymers was shown to improve the flammability of the resulting materials as well. Increased amounts of phosphazene derivative resulted in the reduction of obtained combustion curves and shifting them to higher times of ignition (picture B: compare the reference curve (d) of the phosphazene-free CF_0SF_0 copolymer with curves (e) and (f) of phosphazene-comprising samples $CF_0SF_{0.5}$ and $CF_{0.5}SF_{0.5}$, respectively). The reduction of HRR curves demonstrates that flame is spread slower during material combustion. Similar effects of HACTP concentration on the combustion behavior of crosslinked latex binders were observed also for the other series of emulsion copolymers based on fluorine-free latex particles and particles containing TFEMA only in shell layer. These results are not presented graphically for the sake of simplicity, but the data of ignition times and other evaluated combustion parameters for all the tested samples are listed in Table 4. In all cases it can be stated that the HACTP incorporation and TFEMA copolymerization were found to affect markedly the flame resistivity of latex binders in terms of time to ignition and heat release rate. Nevertheless, it should be noted that all studied

latex binder materials were shown to ignite earlier than the conventional polyethylene binder (see Table 4 and curve (g) in picture B). On the contrary, this drawback is compensated by the decrease in combustion curves of latex binders (demonstrated most significantly in the case of the sample $CF_{0.5}SF_{0.5}$ - curve (f) in picture B), which indicates a slower flame spread during the material combustion.

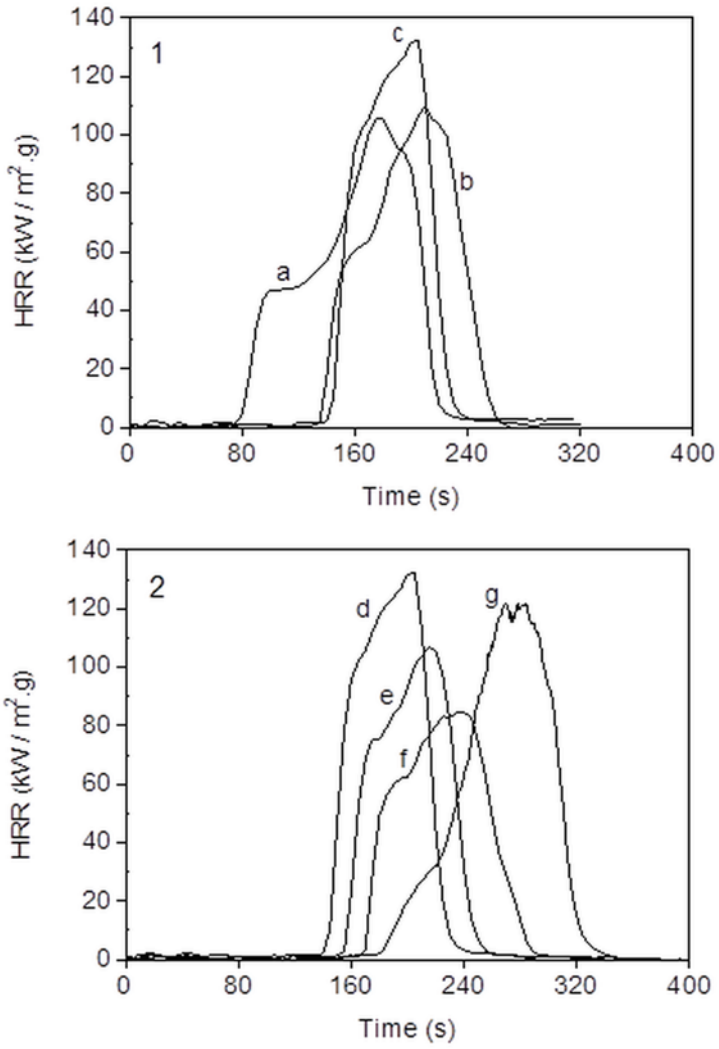

Fig. 8. Comparison of combustion of ADH-crosslinked latex binders. (A) Materials without HACTP flame retardant differing in TFEMA content: (a) copolymer without TFEMA (sample C_0S_0), (b) TFEMA being copolymerized in shell of latex particles (sample C_0SF_0), (c) TFEMA being copolymerized in core and shell layers of latex particles (sample CF_0SF_0). (B) Comparison of materials containing TFEMA in core and shell layers of latex particles and varying in HACTP amount: (d) copolymer without HACTP (sample CF_0SF_0), (e) HACTP incorporated in the shell structure (sample $CF_0SF_{0.5}$), (f) HACTP introduced in core and shell layers (sample $CF_{0.5}SF_{0.5}$). Curve (g) represents combustion of polyethylene.

Table 4

Results of combustion in a dual cone calorimeter for ADH-crosslinked latex binders (containing structured particles differing in the amount and location of HACTP and TFEMA units) in comparison with the conventional polyethylene binder

Evaluated parameter	C_0S_0	$C_0S_{0.5}$	$C_{0.5}S_{0.5}$	C_0SF_0	$C_0SF_{0.5}$	$C_{0.5}SF_{0.5}$	CF_0SF_0	$CF_0SF_{0.5}$	$CF_{0.5}SF_{05}$	Polyethylene
Mean heat release rate[a] ($kW/m^2.g$)	51.1±2.3	36.5±2.0	31.7±0.8	46.4±1.3	37.3±1.6	32.2±1.9	44.8±2.0	35.0±1.7	30.5±1.0	62.3±1.5
Total heat release[a] ($MJ/m^2.g$)	15.1±0.51	9.4±0.36	8.9±0.16	8.6±0.21	8.2±0.34	8.0±0.41	7.0±0.45	6.8±0.42	6.7±0.13	9.0±0.20
Total oxygen consumed[a] (g/g)	1.8±0.02	1.7±0.07	1.6±0.04	1.6±0.09	1.6±0.07	1.5±0.06	1.4±0.07	1.4±0.05	1.3±0.06	2.5±0.04
Total smoke release[a] ($m^2/m^2.g$)	151±4.1	73.9±2.5	62.5±1.1	99.2±2.1	97.0±1.8	97.4±2.1	98.5±3.8	98.7±3.1	97.3±1.5	74.5±3.1
Maximum average rate of heat emission[a] ($kW/m^2.g$)	45.0±2.2	34.1±2.0	33.4±0.7	37.1±1.1	35.2±1.5	34.6±2.0	30.4±1.8	27.5±1.6	24.1±0.8	28.8±0.6
Time to ignition (s)	67±0.2	85±0.5	107±0.3	120±0.1	123±0.7	129±0.6	138±0.4	144±0.6	159±0.5	170±0.4

[a] The evaluated parameter is related to the initial mass of the tested sample.

Table 4 demonstrates that the ADH-crosslinked latex binders comprising increased amount of fluorine and phosphazene groups exhibited lower values of mean heat release rate, total heat release and total oxygen consumed. This phenomenon is more pronounced with the increasing HACTP content in all series of emulsion copolymers and indicates a slower flame spread due to the incorporated HACTP. Decreased values of total smoke release during combustion of fluorine-free samples containing HACTP may reflect a more efficient oxidation of hydrocarbon chains in the presence of the phosphorus compound. It is assumed that the phosphorus atom reacts in the gas phase where the PO• radical is playing the main role.[50] Nevertheless, one of the most important criterions of the flammability evaluation is the maximum average rate of heat emission (MARHE) and value of time to ignition. Both parameters decreased markedly by the growing content of TFEMA and HACTP in the tested binder materials. These results lead us to conclude that HACTP did act as a flame retardant in the investigated latex binders and in the combination with copolymerized TFEMA, materials with sufficient flame stability can be produced via the emulsion polymerization technique. When comparing the resulting binder materials with polyethylene, it can be stated that latex polymers bearing high concentration of TFEMA (around 50 wt.%) and 0.5 wt. % of HACTP in their macromolecular structure are able to exhibit comparable or even better flame resistivity and may represent promising binder materials for different application areas.

3.4 Properties of heterogeneous IEMs

The heterogeneous cation-exchange membranes were easily obtained by dispersing commercial strong acid cation-exchange resin powder in the self-crosslinking latex binder and casting the mixture followed by water evaporation and keto-hydrazide crosslinking reaction proceeding at ambient temperature. The physicochemical and electrochemical properties of the resulting IEMs and a commercial Ralex® heterogeneous cation-exchange membrane were tested from the point of view of water content, IEC, electrical resistance and permselectivity. The results are summarized in Table 5. Dry thickness of the prepared latex-based heterogeneous IEMs was approximately 320–460 μm and thickness of the Ralex® reference membrane was around 210 μm. It was shown that all the latex-based heterogeneous membranes achieved satisfactory physicochemical and electrochemical properties in terms of shape stability, IEC and electric resistance (areal and specific resistance R_A and R_S).

Nevertheless, high-quality heterogeneous IEMs should exhibit sufficiently high values of permselectivity as well. It was found that permselectivity of heterogeneous latex-based IEMs was improved with the increasing amount of TFEMA and HACTP in latex binder copolymers. This phenomenon can be explained by a decreased water uptake of these materials resulting in a restrained transport of aqueous electrolyte solutions through the membrane material. Thus, higher values of areal resistance, specific resistance and permselectivity were probably achieved. Nevertheless, it should be highlighted that only the IEM based on $CF_{0.5}SF_{0.5}$ binder (containing high concentrations of TFEMA and 0.5 wt. % of HACTP in core and shell structures of latex particles) was shown to be fully comparable with the commercial Ralex® membrane and was able to meet the requirements for general purpose heterogeneous cation-exchange membranes.

Table 5

Physicochemical and electrochemical properties of heterogeneous IEMs based on ADH-crosslinked latex binders in comparison with the commercial Ralex® CM(H) heterogeneous cation-exchange membrane

Evaluated parameter	C_0S_0	$C_0S_{0.5}$	$C_{0.5}S_{0.5}$	C_0SF_0	$C_0SF_{0.5}$	$C_{0.5}SF_{0.5}$	CF_0SF_0	$CF_0SF_{0.5}$	$CF_{0.5}SF_{05}$	Ralex®	Limit value[a]
Difference in swelled thickness (wt.%)	30.5±1.9	42.2±2.6	33.1±2.1	25.2±1.8	28.4±1.2	27.6±2.5	24.5±1.1	23.2±2.0	21.8±1.8	35.8±1.2	<65
IEC (meq/g)	2.98±0.05	2.83±0.01	2.67±0.02	2.60±0.02	2.55±0.05	2.90±0.03	2.74±0.04	2.62±0.01	2.81±0.03	2.99±0.03	>2.2
R_A ($\Omega.cm^2$)	1.34±0.06	1.58±0.33	1.50±0.15	1.58±0.29	1.96±0.11	1.79±0.03	2.54±0.25	2.67±0.17	2.93±0.01	2.68±0.05	<8.0
R_S ($\Omega.cm$)	35.8±0.6	36.1±1.1	28.2±0.9	40.5±2.4	37.7±0.7	42.7±0.14	49.8±1.4	54.8±0.4	61.1±0.8	94.4±0.6	<120
P (%)	67.3±2.5	64.2±1.3	67.3±1.4	76.2±2.7	72.4±1.1	75.7±2.0	85.9±0.5	89.0±1.6	90.6±0.8	92.9±0.4	>90

[a] Information given by the manufacturer of Ralex® standard membranes for general purpose.

4. Conclusions

In the present work, we focused on self-crosslinking latexes based on keto-hydrazide crosslinking system and their application as alternative binder materials for easily fabricated heterogeneous ion-exchange membranes. The self-crosslinking acrylic core–shell latexes comprising copolymerized 2,2,2-trifluorethyl methacrylate and hexaallylamino-*cyclo*-triphosphazene were successfully prepared by the semi-continuous non-seeded emulsion polymerization and the heterogeneous cation-exchange membranes were obtained by mixing commercially available cation-exchange particles in the self-crosslinking latex and casting the mixture followed by air-drying at room temperature. It was found that the increased concentration of fluorine atoms and phosphazene units in the macromolecular structure of crosslinked latex binders resulted in a significant enhancement of their flame resistance and shape stability in aqueous environment. Moreover, the easily prepared heterogeneous cation-exchange membranes based on emulsion core–shell copolymers with higher amounts of fluorine and phosphazene units were shown to exhibit physicochemical and electrochemical properties comparable to a commercial heterogeneous cation-exchange Ralex® membrane. Thus, it can be concluded that water-borne one-component thermosetting binder systems with increased flame stability and enhanced water resistance were developed, having a potential application as binder materials for heterogeneous cation-exchange membranes.

Acknowledgements

The work was carried out within the framework of project No. LO1418 "Progressive development of Membrane Innovation Centre" supported by the program NPU I Ministry of Education Youth and Sports of the Czech Republic, using the infrastructure of the Membrane Innovation Centre.

References

1. Xie, K., Hou, A., Shi, Y. *J. Appl. Polym. Sci.* **2008**, *108*, 1778–1782.

2. He, L., Liang, J., Zhao, X., Li, W., Luo, H. *Prog. Org. Coat.* **2010**, *69*, 352–358.

3. An, Q., Xu, W., Hao, L., Huang, L. *J. Appl. Polym. Sci.* **2013**, *127*, 1519–1526.

4. Yu, M., Zhang, B., Deng, B., Yang, X., Sheng, K., Xie, L., Lu, X., Li, J. *J. Appl. Polym. Sci.* **2010**, *117*, 3575**–**3581.

5. Ling, H., Junyan, L. *J. Fluorine Chem.* **2008**, *129*, 590–597.

6. Xu, W., An, Q., Hao, L., Huang, L. *J. Appl. Polym. Sci.* **2012**, *125*, 2376–2383.

7. Fisher, B., Autenrieth, T., Wagner, J. *Langmuir* **2010**, *26*, 6201–6205.

8. Zheng, W., He, L., Liang, J., Chang, G., Wang, N. *J. Appl. Polym. Sci.* **2011**, *120*, 1152–1161.

9. Xiao, X., Xu, R. *J. Appl. Polym. Sci.* **2011**, *119*, 1576–1585.

10. Chen, Y., Lina, D. *Polym. Prep.* **2007**, *48*, 325–326.

11. Chen, Y., Zhang, Ch., Chen, X. Eur. Polym. J. **2006**, *42*, 694–701.

12. Cui, X., Zhong, S., Wang, H. *Colloid Surf. A: Physicochem. Eng. Aspects* **2007**, *303*, 173–178.

13. Cheng, S. Y., Chen, Y. J., Chen, Z. G. *J. Appl. Polym. Sci.* **2002**, *85*, 1147–1153.

14. Ha, J. W., Park, I. J., Lee, S. B., Kim, D. K. *Macromolecules* **2002**, *35*, 6811–6818.

15. Shah, B. G., Shahi, V. K., Thampy, S. K., Rangarajan, R., Ghosh, P. K. *Desalination* **2005**, *172*, 257–265.

16. Nagarale, R. K., Gohil, G. S., Shahi, V. K. *Adv. Colloid Interface Sci.* **2006**, *119*, 97–130.

17. Khodabakhshi, A. R., Madaeni, S. S., Hosseini, S. M. *Sep. Purif. Technol.* **2011**, *77*, 220–229.

18. Hosseini, S. M., Madaeni, S. S., Heidari, A. R., Amirimehr, A. *Desalination* **2012**, *284*, 191–199.

19. Martí-Calatayud, M. C., Buzzi, D. C., García-Gabaldón, M., Bernardes, A. M. *J. Membr. Sci.* **2014**, *466*, 45–57.

20. Kariduraganavar, M. Y., Nagarale, R. K., Kittur, A. A., Kulkami, S. S. *Desalination* **2006**, *197*, 225–246.

21. Gohil, G. S., Shahi, V. K., Rangarajan, R. *J. Membr. Sci.* **2004**, *240*, 211–219.

22. Xu, T. *J. Membr. Sci.* **2005**, *263*, 1–29.

23. Gizli, N., Cinarli, S., Demircioglu, M. *Sep. Purif. Technol.* **2012**, *97*, 96–107.

24. Vyas, P. V., Shah, B. G., Trivedy, G. S., Ray, P., Adhikary, S. K., Rangarajan, R. *J. Membr. Sci.* **2001**, *187*, 39–46.

25. Vyas, P. V., Shah, B. G., Trivedy, G. S., Ray, P., Adhikary, S. K., Rangarajan, R. *React. Funct. Polym.* **2000**, *44*, 101–110.

26. Hosseini, S. M., Askari, M., Koranian, P., Madaeni, S. S., Moghadassi, A. R. *J. Ind. Eng. Chem.* **2014**, *20*, 2510–2520.

27. Nagarale, R. K., Shahi, V. K., Thampy, S. K., Rangarajan, R. *React. Funct. Polym.* **2004**, *61*, 131–138.

28. Wang, M., Wang, X., Jia, Y., Liu, X. *Desalination* **2014**, *351*, 163–170.

29. Hosseini, S. M., Madaeni, S. S., Khodabakhshi, A. R. *J. Membr. Sci.* **2010**, *351*, 178–188.

30. Bouzek, K., Moravcová, S., Schauer, J., Brožová, L., Pientka, Z. *J. Appl. Electrochem.* **2010**, *40*, 1005–1018.

31. Hosseini, S. M., Rahzani, B., Asiani, H., Khodabakhshi, A. R., Hamidi, A. R., Madaeni, S. S., Moghadassi, A. R., Seidypoor, A. *Desalination* **2014**, *345*, 13–20.

32. Philamore, H., Rossiter, J., Walters, P., Winfield, J., Ieropoulos, I. *J. Power Sources* **2015**, *289*, 91–99.

33. Lin, R., Chen, B., Chen, G., Wu, J., Chiu, H., Suen, S. *J. Membr. Sci.* **2009**, *326*, 117–129.

34. Zhong, S., Cui, X., Dou, S., Liu, W. *J. Power Sources* **2010**, *195*, 3990–3995.

35. Li, H., Kan, Ch., Du, Y., Liu, D. *Polym. Prep.* **2002**, *43*, 413–414.

36. Zhang, S. F., Liu, F. R., He, Y. F., Wang, R. M., Song, P. F. *Arab. J. Sci. Eng.* **2014**, *39*, 23–30.

37. Zhang, S. F., He, Y. F., Wang, R. M., Wu, Z. M., Song, P. F. *Iran Polym. J.* **2013**, *22*, 447–456.

38. Koukiotis, Ch. G., Karabela, M. M., Sideridou, I. D. *Prog. Org. Coat.* **2012**, *75*, 106–115.

39. Koukiotis, Ch., Sideridou, I. D. *Prog. Org. Coat.* **2010**, **69**, 504–509.

40. Zhang, X., Liu, Y., Huang, H., Li, Y., Chen, H. *J. Appl. Polym. Sci.* **2012**, *123*, 1822–1832.

41. Benziger, J. B., Chia, S.Y., De Decker, E., Kevrekidis I. G. *J. Phys. Chem. C* **2007**, *111*, 2330–2334.

42. Iwai, Y, Yamanishi T. Polym. Degrad. Stab. **2009,** 94, 679–687.

43. Crotty, D. US Patent US 6,391,177 B1 **2002**.

44. Machotova, J., Zarybnicka, L., Bacovska, R., Vrastil, J., Hudakova, M., Snuparek, J. *Prog. Org. Coat*. **2016**, *101*, 322−330.

45. Fox, T. G., Flory, P. J. *J. Appl. Phys.* **1950**, *21*, 581−591.

46. Rychlý, J., Hudáková, M., Rychlá, R. *J. Therm. Anal. Calorim.* **2014**, *115*, 527−535.

47. Zhong, S., Cui, X., Dou, S., Liu, W. *J. Power Sources* **2010**, *195*, 3990−3995.

48. Pi, P., Wang, W., Wen, X., Xu, S., Cheng, J. *Prog. Org. Coat.* 2015, *81*, 66−71.

49. Šňupárek, J., Bidman, A., Hanuš, J., Hájková, B. *J. Appl. Polym. Sci.* **1983**, *28*, 1421−1428.

50. Schartel, S. *Materials* **2010**, *3*, 4710−4745.